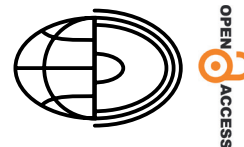


Genetic map of the Wielka Żuława soil cover: blanks to be filled using existing cartographic materials and remote-sensing data



Marcin Świtoniak*^a, Paweł Radomski, Julia Dziczek,
Marcin Sykuła, Maciej Markiewicz

Nicolaus Copernicus University in Toruń, Department of Soil Science and Landscape Ecology, Lwowska 1, 87-100, Toruń, Poland

*E-mail: swit@umk.pl

^a<https://orcid.org/0000-0002-9907-7088>

Abstract. Poland is considered to have a very well mapped soil cover and detailed soil cartographic materials. Despite this, some areas have “blank spots” on soil-agricultural or soil-habitat maps. These include the Wielka Żuława island on Jeziorak Lake (on the Łąwa Plain). This island is almost deserted and inaccessible, making detailed field research there very difficult. The aim of the work was to check the possibility of using existing cartographic materials and remote-sensing data to develop a genetic map of the soils of this area. In order to interpret the existing materials, preliminary field works were carried out: six soil pits and 22 manual drillings to an average depth of 2 m. These studies showed significant diversity of soil cover. The largest share within the central, upland part of the island have autogenous rusty soils (Brunic Arenosols according to the World Reference Base [WRB]) and clay-illuvial soils (Luvisols – WRB). The lower locations (mainly along the coast of the island) were dominated by organic soils (Histosols – WRB). The digital elevation model (DEM) enables precise determination of the boundary between THE mentioned autogenous and hydrogenic soils. In the group of organic pedons, a large area was degraded, which was expressed by the occurrence of murshic soils (Murshic Histosols – WRB). The DEM obtained from LiDAR data shows networks of (almost invisible in aerial photos) drainage ditches and channels, which turned out to be very useful in determining the extent of the mentioned degradation. The greatest difficulties concerned the extent of soil developed as a result of human influence – colluvial (Solimovic Arenosols) and anthropogenic soils. In the first case, a relief model combined with archival orthophotomosaics allowed for an approximate estimation of the places where these soils occur. Both elements (DEM and archival aerial photos) were also used to estimate the extent of occurrence of technogenic soils (Technosols – WRB).

Key words:
LIDAR data,
orthophotomosaic,
soil cartography,
Polish Soil Classification,
World Reference Base for Soil
Resources

Introduction

The soil cover of Poland was mapped in detail already in the 1950s and 1960s, when large-scale fieldwork was carried out to create the first maps covering almost the entire country. In this period, agricultural soil maps on a scale of 1:5,000 and 1:25,000 were developed (Witek 1965). Even though they were

created according to a nomenclature that is now outdated, the information contained in these maps allows for their quite precise updating to modern, currently applicable classification systems (Świtoniak et al. 2019; Kabała et al. 2022). On the other hand, it should be noted that most agricultural areas have not been verified in terms of the spatial extent of individual soil contours since the 1950s/1960s. Much more up-to-date and detailed data are available for

the soil cover of forests managed by the State Forests. The soil-habitat maps prepared by this institution on a scale of 1:5,000 are constantly updated (every 20–25 years) and are currently based on the relatively modern Classification of Forest Soils in Poland (2000). The reclassification of these maps to the latest version of the Polish Soil Classification (2019) does not pose any major difficulties (Kabała et al. 2022).

Despite such accurate mapping of Poland's soil cover, most of the contours require re-verification. Since the 1970s, many scientific works have appeared discussing the need to implement aerial and satellite photos when delineating and updating the contours of soil units (e.g., Buringh 1970; Białousz 1978; Białousz et al. 1978; Malik et al. 1984; Akamigbo et al. 1994; Sinkiewicz 1998; Žížala et al. 2019). Moreover, these photos provide very good results in determining the spatial extent of completely eroded soils – calcareous Regosols within moraine plateaus in glacial moraine regions (Matecka and Świtoniak 2020) or other soil units (e.g., eroded Luvisols) transformed by anthropogenic denudation (Świtoniak et al. 2013).

Detailed, high-resolution Digital Terrain Models (DTMs) are a breakthrough tool in cartography. Currently, models generated from LiDAR (Light Detection And Ranging) data are very often used. Some of the many interesting examples of the use of LiDAR are the estimation of leaf area index (LAI) using ALS data (Sabol et al. 2014). LiDAR-based DTMs offer enormous interpretative and analytical possibilities. These models are used for analyses of slope inclination and exposure, surface runoff, delineation of degradation (erosional truncation) and aggradation (colluvium accumulation) zones, and many other purposes. Thanks to their high resolution, they reveal surface features invisible to the naked eye, such as drainage ditches hidden under the tree canopy, which are not shown in a regular aerial photo. Based on LiDAR scans from before and after a fire, it is also possible to estimate losses in organic soils and carbon dioxide emissions during the combustion process (Reddy et al. 2015). The great advantage of LiDAR-based models is their enormous interpretative possibilities, which in the field of soil science can also support farmers in preventing soil degradation due to salinity (De Feudis et al. 2021). In more extreme conditions, various forms of erosion – including those related to mass movements – can be monitored by “LiDAR monitoring” even in places where in-situ testing is impossible. By performing several LiDAR aerial surveys, it is possible to create a

series of maps with the historical course of colluvium deposition, which in turn can support the authorities' decision-making in connection with crisis response (Domlija et al. 2019).

In recent years, there has been a rapid development in the industry of unmanned aerial vehicles (UAVs), popularly called “drones”. These allow surveyors to take very accurate and low-cost LiDAR measurements and aerial photography in relatively small areas. This is particularly useful, or even necessary, when conducting detailed studies of dynamic and local environmental changes, such as mass movements (Jong-Tae et al. 2023) or the shifting of glaciers (Baurley et al. 2022) or dunes (Solazzo et al. 2018), or when assessing losses after natural disasters. In the study of the variability of soil cover properties, UAVs have been used to, among other things, determine changes in soil organic matter content (Zhou et al. 2023) or in other aspects of precise agriculture (Gevaert et al. 2015).

As shown above, since the creation of soil-agricultural and soil-habitat maps, many technologies that enable the updating of spatial soil data have been developed. Moreover, on soil-genetic maps – even detailed ones – there are individual forest or rural areas for which no information relating to soil is recorded. Such exceptions include the area of Wielka Żuława island. Although a technical soil classification of land (tax-bonitation survey) was carried out on this island in 1966, both on medium- and larger-scale overview soil-genetic maps and detailed soil-agricultural/-habitat maps, the area of the island is a “blank spot” in terms of soil cover information. Therefore, the aim of this work is to use cartographic and remote-sensing materials in the development of a genetic map of the soils of Wielka Żuława island. To achieve the above goal, the following research tasks were distinguished:

- a review of existing cartographic materials – topographic maps, surface geological maps,
- -field studies of genetic variability of soils in the studied area,
- classifying of soils according to modern systems – 6th edition of the Polish Soils Classification (PSC, 2019) and the newest version of World Reference for Soil Resources (WRB – IUSS, 2022).
- the use of an orthophotomosaic and digital terrain model (DTM) elaborated on LiDAR data in determining the spatial range of individual soil units.

2. Study area and methods

The research was conducted in the area of Wielka Żuława in the southern part of Lake Jeziorak (Fig. 1). It is an inland island with an elongated shape and total area of 82.4 ha, which makes it the largest island in Jeziorak and one of the largest in Poland. The island is located within the administrative boundaries of the city of Iława in the south-western part of the Warmian-Masurian Voivodeship.

Wielka Żuława is located in a moist and cool temperate climate zone (IPCC 2006). According to the Köppen–Geiger Climate Classification, the region is located in a fully humid zone with temperate and warm summer (Kottek et al. 2006). Average annual air temperature (based on data from the period 1991–2020) varied between 8 and 8.5 °C, and the average annual precipitation is ~550–600 mm, with the majority of precipitation occurring in summer season (Tomczyk and Bednorz 2022). The humid period (predominance of precipitation over potential evaporation) lasts for the whole year, conditioning the leaching soil-water regime in pedons with good natural drainage (autogenic soils).

In morphogenetic terms, the island is a kame hill (Fig. 2) located in the bottom of a tunnel valley created during the Pomeranian phase (16–17 kyr BP) of the Weichselian glaciation (Marks 2012) and filled by the waters of Lake Jeziorak. The main part of the island has the form of a relatively flat kame plateau with steep slopes, the inclination of which exceeds 20° in the eastern and south-eastern parts of the island. In other parts, slopes with an inclination of about 10° predominate. These slopes have a relative height of over 10 m and arise from ~100 m a.s.l. (the average water level is 99.2 m a.s.l.) to the highest point at 116.6 m a.s.l. According to the geological map (source), the kame hill is composed of sediments of varying texture – from sand to loam. In the northern and southern parts of the island only, there are relatively small areas of biogenic plains that rise slightly above the lake's water surface and cover sandy fluvoglacial sediments.

Until the late 1960s, most of the island was still used for agriculture (Fig. 3). Archival aerial photographs show a significant share of arable land, especially in the central part of the island. Only the slopes adjacent to the lake and the

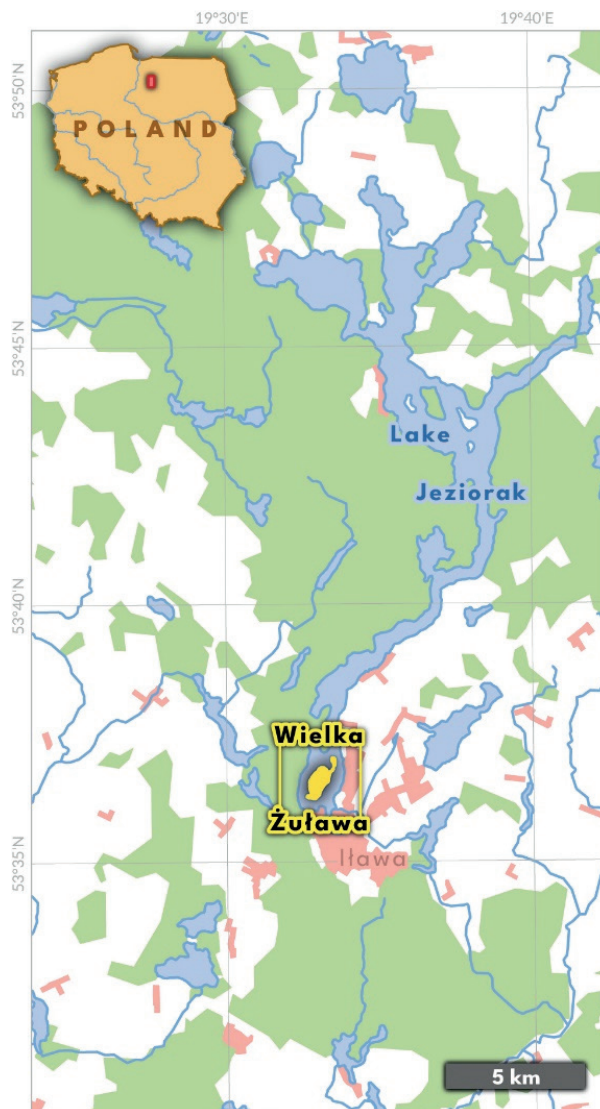


Fig. 1. Location of Wielka Żuława island

northern and southern marshy areas were covered with forests. In the eastern and southern parts of the island, there were also tourist and recreation resorts. Currently, most of the island is fallow and overgrown with shrubs and trees (mainly hawthorn and other deciduous species). A few tourism resorts still operate along the eastern coast.

Fieldworks were conducted in November 2022. Six soil pits and 22 manual augerholes (Tables 1 and 2; Figs 4 and 5) were made. Soil samples were taken from the genetic horizons described in soils represented by four soil pits. Disturbed soil samples were taken from every genetic soil horizon.

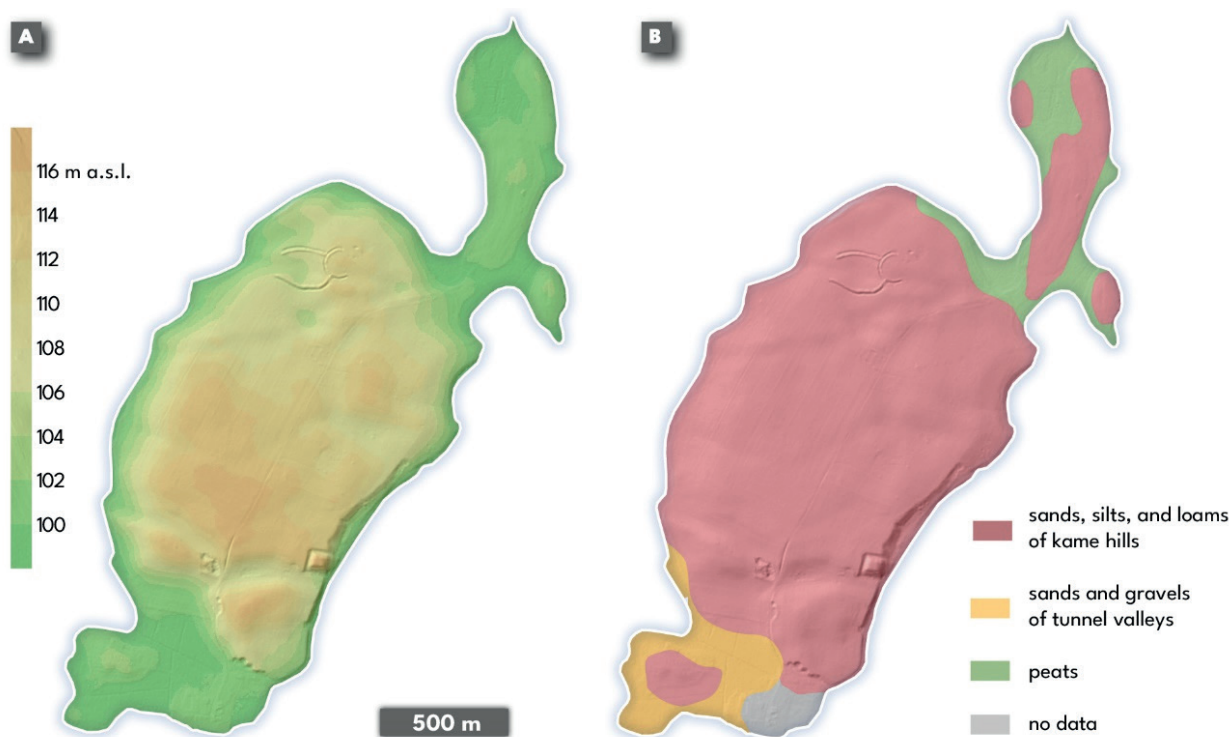


Fig. 2. Maps of relief (left) and geological surface formations of Wielka Żuława (right)

3. Results

Standard soil analyses were performed using the following methods: particle-size distribution by sieve and sedimentary aerometric method; content of total carbon (TC) and total nitrogen (TN) by dry combustion (VarioMacroCube, Elementar, Langensfeld, Germany), following which the TC content was corrected with content of inorganic carbon to determine the total organic carbon content (TOC); calcium carbonate (CaCO_3) content by volumetric Scheibler method; and pH of soil-to-solution ratio of 1:2.5 using 1 M KCl and distilled H_2O as the suspension medium. Colour was described according to Munsell Soil Color Charts (2000).

The systematic position and names of diagnostic horizons were given after the sixth edition of the Polish Soil Classification (PSC 2019) and WRB (IUSS Working Group WRB 2022), while the symbols of horizons were given solely after WRB. English names of soil units (PSC 2019) were given according to proposal of Kabala et al. (2019).

The investigated soils can be divided into three main groups depending on the differentiation in natural conditions in the context of their water regime. The largest group (15 profiles) consists of well-drained mineral (autogenic) soils supplied mainly by rain-water and with good natural drainage conditions. They were derived mainly from kame sediments with the texture of sands/loamy sands or sands underlain by loamy materials. In the first case of deep (thicker than 200 cm) sands, rusty soils with diagnostic sideric horizon (PSC 2019) were developed (WRB 2022 – Brunic Arenosols). In the second case, the cover sands also usually had well-developed Bw horizons (sideric horizon in PSC and expressed by Brunic qualifier in WRB), but in the upper part of the deeper-lying (starting 50–200 cm from surface) loamy material an illuvial horizon of clay accumulation – argic (Bt) was also noted. If the upper boundary of the Bt horizon starts at ≤ 100 cm, the soils were classified as clay-illuvial (PSC 2019) and as Luvisols (WRB 2022), and in

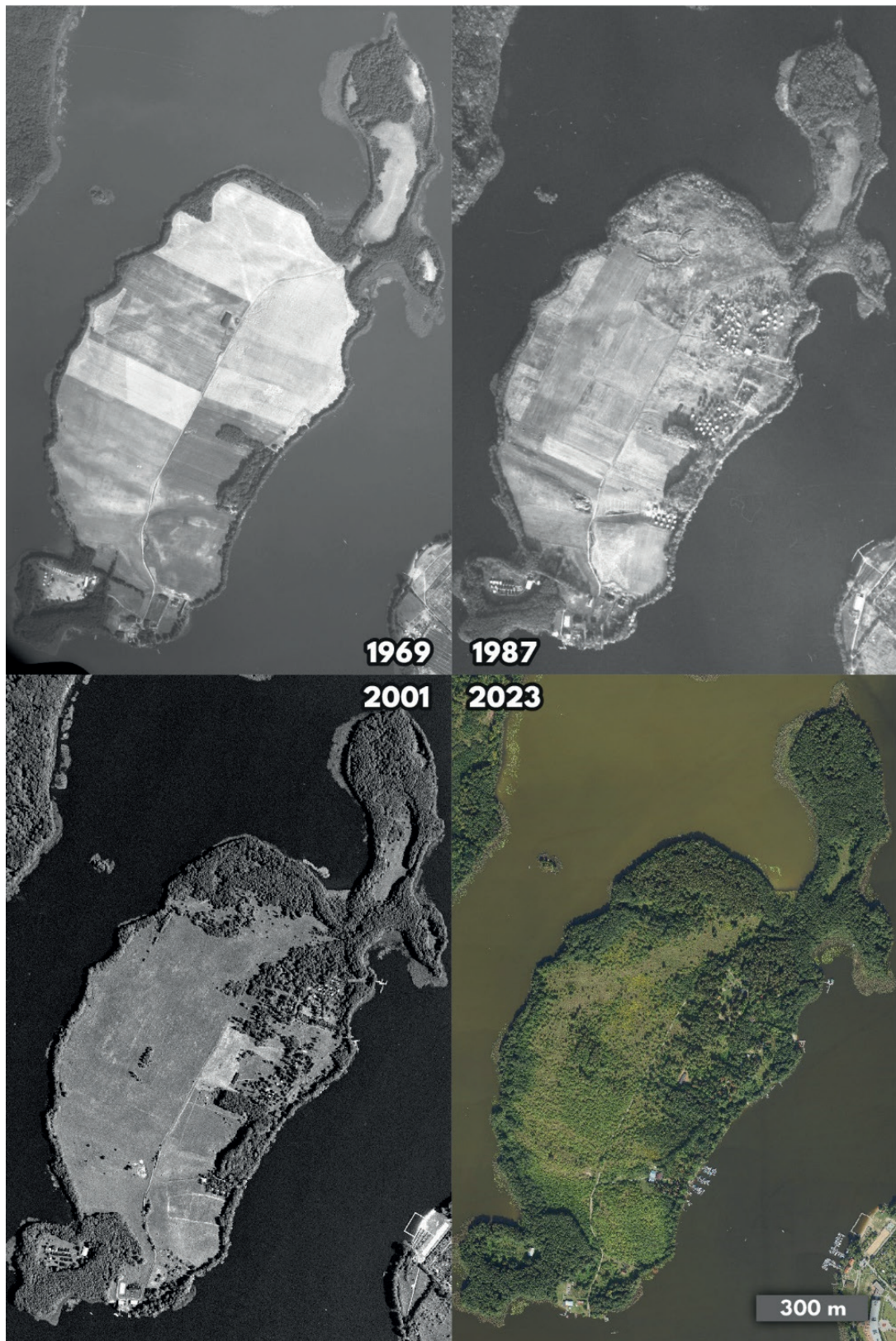


Fig. 3. Wielka Żuława island on a compilation of archival aerial photos – orthophotomosaics

deeper cases (>100 cm from surface) as rusty soils (or Brunic Arenosols – WRB). In clay-illuvial soils (WRB – Luvisols), the lithological discontinuity between sands and loams was accompanied by a sudden increase in the clay fraction (in the Bt top), which was expressed by the subtype “texturally contrasted” (PSC 2019) or the qualifier “Endoabruptic” (WRB 2022). Common in both types of soils (clay-illuvial and rusty soils) were features connected with ploughing expressed by a clearly homogenised A horizon with a sharp boundary at a depth of 30 cm. Such thickness of humus horizons causes these soils to be assigned the subtype “humic” (PSC 2019). However, the humus content was too low to apply the Humic qualifier in WRB (2022). Locally, occurrences were also found of truncated, erosionally shallowed (Phillips et al. 1999; Świtoniak et al. 2016) clay-illuvial soils (WRB – Haplic Luvisol) (in augerhole 21) and ordinary colluvial soils (WRB – Solimovic Arenosols) developed from humic slope materials (in augerhole 6). Colluvial soils were characterised by a relatively weakly developed but thick A horizon (Świtoniak 2015; Zádorová et al. 2023).

The second group based on natural water regime contained poorly drained mineral soils strongly influenced by groundwater. These soils had well-developed, humus-rich, dark and thick A horizons and parent materials with pronounced gleyic properties. Mostly they were classified as

typical black earths (PSC 2019) and according to WRB (2022) as Endogleyic Phaeozems or Gleysols. This group also included turbisols (PSC 2019) and Phaeozems with qualifier “Relocatic” (WRB 2022) that were strongly mixed by humans to great depth, mainly in the areas of former recreation centres. The soils belonging to the poorly drained group were located at low altitudes, mainly near the shores of the island, and were formed from kame or fluvio-glacial sediments ranging from coarsely textured gravels or sands to loams.

The last group consisted of organic soils, with the lowest ones being located directly above the current water table of Jeziorak. Originally, these soils developed through the accumulation of peat at a very shallow water table. Currently, most of them show clear signs of drainage degradation – black, granular mursh is visible in the uppermost part of pedons. In the WRB classification, all of these soils were classified as Murshic Histosols. In the Polish Soil Classification (2019), the thickness of the mursh determined their differentiation into two types – murshic soils if it was at least 30 cm thick; and murshic peat soils if it did not exceed 30 cm. In one case, the mursh was covered by 30-cm-thick mineral material, probably deliberately added by the previous owners (now it is covered by forest) in order to improve the functional properties of this soil.

Table 1. Selected properties of investigated soils (soil pits)

Horizon	Sampling depth [cm]	OC	Nt	C/N	CaCO ₃ [%]	pH		Colour*		Fraction [%]			Class USDA
		[%]				H ₂ O	1M KCl	dry	moist	Sand 2-0.05 mm	Silt 0.05-0.002 mm	Clay<0.002 mm	
9 SP Humic brown-rusty soil													
Ap	0-30	0.87	0.08	11	n.d.	5.5	4.2	10YR 7/2	10YR 3/3	75	17	8	SL
A	30-55	0.52	0.05	11	n.d.	5.4	4.5	10YR 7/2	10UR 3/3	77	19	4	LS
Bw	55-90	0.21	0.02	10	n.d.	5.5	4.5	10YR 7/4	10YR 4/4	79	17	4	LS
C(g)	90-130	n.d.	n.d.	n.d.	n.d.	6.0	4.8	n.d.	n.d.	90	9	1	S
2Bt	130-150	0.11	0.02	5	n.d.	6.0	4.6	n.d.	n.d.	67	17	16	SL
18 SP Murshic fibric peat soil													
Ha	0-25	40.7	2.83	14	n.d.	5.8	5.5	10YR 3/3	10YR 2/2	n.d.	n.d.	n.d.	n.d.
Hi	25-70	33.2	1.98	17	n.d.	5.6	5.6	10YR 3/4	10YR 2/2	n.d.	n.d.	n.d.	n.d.
25 SP Typical black earth													
Ap	0-30	2.26	0.21	11	2.16	7.1	7.0	10YR 4/2	10YR 3/1	79	15	6	LS
Ckl	30-110	n.d.	n.d.	n.d.	12.4	8.4	8.3	n.d.	n.d.	95	3	2	S
28 SP Earth-covered murshic soil													
A	0-30	4.53	0.32	14	n.d.	6.2	6.1	5Y/4/1	10YR/2/1	92	3	5	S
Ha	30-100	41.5	2.87	14	n.d.	5.4	5.1	5Y/3/1	10YR2/1	n.d.	n.d.	n.d.	n.d.

Table 2. Classification of soils (soil pits and augerholes)

Nr	Soil subtype (PSC 2019)	RSG (WRB 2022)	Horizon sequence	D	Elevation m a.s.l.	Terrain
1	Typical black earth	Endogleyic Phaeozem	A-Al-Cr	PD	100.03	flat
2	Typical black earth	Mollic Gleysol	A-Cl-Cr	PD	100.71	flat
3	Turbisol	Phaeozem (Relocatic)	A	PD	99.94	flat
4	Humic texturally contrasted clay-illuvial soil (rustic)	Endoabruptic Luvisol (Neobrunic)	A(p)-Bw-Eg-2Bt-2BC	WD	111.65	medium slope
5	Typical clay-illuvial soil	Epiabruptic Luvisol	A-Eg-2Bt	WD	116.50	summit
6	Humic ordinary colluvial soils	Solimovic Arenosol	A-A-A-Al	WD	107.22	depression
7 SP*	Brown-rusty soil	Brunic Arenosol (Protoargic)	A-Bw-B(t,g)-C	WD	111.47	medium slope
8	Humic rusty soil	Brunic Arenosol	A(p)-Bw-C	WD	116.10	flat
9 SP	Humic brown-rusty soil	Brunic Regosol	A(p)-A-Bw-Eg-2Bt	WD	112.85	flat
10	Humic texturally contrasted clay-illuvial soil (rustic)	Endoabruptic Luvisol (Neobrunic)	A(p)-Bw-2Bt(g)-2C	WD	113.62	flat
11	Humic texturally contrasted clay-illuvial soil (rustic)	Endoabruptic Luvisol (Neobrunic)	A(p)-Bw-2Bt(g)-2C	WD	115.00	flat
12	Humic rusty soil	Brunic Arenosol	A(p)-A-Bw-Eg-2Bt	WD	112.30	flat
13	Turbisol	Endogleyic Phaeozem (Relocatic)	A-Cl	WD	102.84	flat
14	Typical black earth	Endogleyic Phaeozem	A-Cl-Cr	PD	100.55	flat - terrace
15	Humic texturally contrasted clay-illuvial soil (rustic)	Endoabruptic Luvisol (Neobrunic)	A-Bw-2Bt	WD	109.89	flat
16	Humic rusty soil	Brunic Arenosol	A(p)-Bw-C	WD	111.03	flat
17	Typical black earth	Endogleyic Phaeozem	A-Al-Cr	PD	99.97	flat
18 SP	Murshic fibric peat soil	Murshic Fibric Histosol	Ha-Hi	VPD	99.47	flat - shore
19 SP	Humic rusty soil	Brunic Arenosol	Ap-Bw-C-Cl	WD	101.29	summit of hill
20	Sapric Histosol	Sapric Histosol	Ha-Cr	VPD	99.92	flat depression
21	Eroded humic clay-illuvial soil	Haplic Luvisol	A-Bt-Ckg-Cl	WD	101.45	small hill
22	Typical black earth	Endogleyic Phaeozem	A-Al-Cr	PD	100.25	small hill
23	Brown-rusty soil	Brunic Arenosol (Protoargic)	A-Bw-B(t,g)-C	WD	109.64	flat
24	Murshic soil	Murshic Histosol	Ha-Cr	VPD	100.08	almost flat
25 SP	Typical black earth	Mollic Gleysol	Ap-Clk	PD	101.04	flat
26	Typical black earth	Mollic Gleysol	A-Cr	PD	100.29	almost flat
27	Murshic soil	Murshic Histosol	Ha-Cr	VPD	99.32	flat
28 SP	Earth-covered murshic soil	Murshic Histosols (Novic)	A-Ha	VPD	100.04	flat



Fig. 4. Morphology of investigated profiles (soil pits)

4. Discussion

A detailed mapping of the soil cover (to create a map on a scale of 1:5,000) of the investigated area would be very time-consuming. An environment with such significant pedodiversity would require a much larger number of soil pits and augerholes (Polskie Stowarzyszenie Klasyfikatorów Gruntów 2020). However, the research carried out allowed for the detection of the main relationships between the main environmental components and soil variability.

The creation of a genetic map of the soils allowed not only a relatively precise determination of the range of individual soil units but also an estimation of their share in the area of the entire island.

The main part of the island's surface is covered by soil contours with good natural drainage, corresponding in extent to the same plateau occupying the central part of the study area and small elevations located in its northern and southern

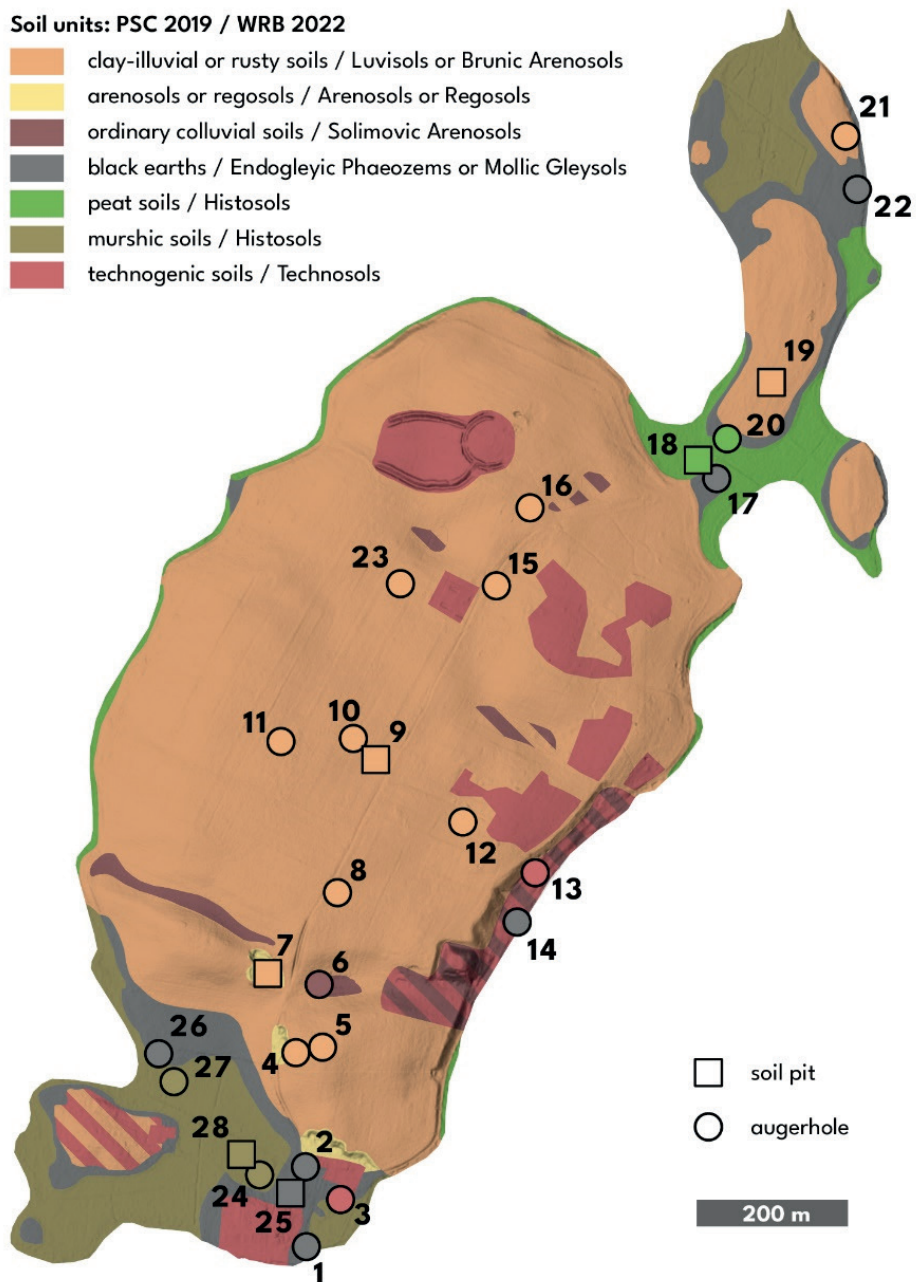


Fig. 5. Map of soil cover of Wielka Żuława island

parts (Fig. 5). These areas are dominated by clay-illuvial soils (PSC 2019) / Luvisols (WRB 2022) and rusty soils (PSC 2019) / Brunic Arenosols (WRB 2022). Both types of soils create a complex mosaic depending on the thickness of the sandy cover and depths to the upper limit of Bt horizons. This variability is not reflected in any surface features of the environment, such as relief, colour of surface horizons, or variability of vegetation. For this reason,

it is not possible to separate these two soil units based on other cartographic materials, and they have been marked on the map as a soil association. A similar problem has already been described in the Brodnica Lake District (Świtoniak 2006). Nevertheless, the soil types have similar utility value due to their cover sands being underlain by loamy textured material (Świtoniak 2007). Part of the surface of the studied kames is characterised by a distinctive inclination of

Table 3. Share of area of individual soil units

Soil unit PSC 2019 / WRB 2022	Surface [m ²]	Share [%]
Clay-illuvial and rusty soils / Luvisols and Brunic Arenosols	551,727	65.7
- with colluvial soils / with Solimovic Arenosols	6,260	0.7
- with technogenic soils / with Technosols	10,210	1.2
Colluvial soils / Solimovic Arenosols	6,417	0.8
- with technogenic soils / with Technosols	19,283	2.3
Murshic soils / Histosols	80,003	9.5
Black earths / Endogleyic Phaeozems and Mollic Gleysols	64,255	7.6
Technogenic soils	59,336	7.1
Peat soils / Histosols	37,973	4.5
Arenosols and regosols / Arenosols and Regosols	4,655	0.6
Sum	840,120	100.0

slopes, which, combined with arable use in the past, must have led to a significant erosion of the soil cover (Kobierski 2013; Podlasiński 2013; Świtoniak 2014). Field studies confirmed the truncation of some clay-illuvial and rusty soils. The occurrence of colluvial deposits in some depressions was also proven.

The extend of eroded and colluvial soils can be easily determined using aerial photos showing the variability of colour of surface horizons (Świtoniak et al. 2013; Żiżala et al. 2019; Matecka and Świtoniak 2020; Radziuk and Świtoniak 2022), especially in combination with interpretation of the terrain model. It would also be very useful to use vegetation cover images enabling the calculation of NDVI (Singh et al. 2004). Such remote-sensing materials cannot be used in the analysed area. The entire island is overgrown with secondary succession vegetation (Fig. 3), which is completely independent of the degree of erosional transformation of soils. The latest photos showing the colour of surface horizons are panchromatic and come from the 1980s, which makes it impossible to use them in assessing the extent of eroded or colluvial soils.

For the above reasons, the only material helpful in estimating the occurrence of erosionally transformed soils (in this case colluvial soils) was a map showing the locations of potential surface runoff (Fig. 6) developed on the basis of the DTM generated from LiDAR data. The soil map does not take into account the potential occurrence of colluvial soils in places that in the past were not used for agriculture (having

instead been covered with forests), which indicates the lack of possibility of intensive movement of slope sediments. This applies mainly to the foot of the kame plateau slopes near the lake shores. LiDAR data have already been used many times by other authors to study soil erosion (e.g., Gunay et al. 2019; Domlija 2019).

During the field reconnaissance, individual places (0.6%) of former sand and gravel excavations were also confirmed; in these places, the soil was completely destroyed and currently there are poorly formed arenosols and regosols.

An important issue is to determine the boundary between the above-described well-drained autogenic soils and mineral semihydrogenic soils strongly influenced by groundwater. In the case of the studied island, the occurrence of semihydrogenic soils was found only in low-lying areas along the shores of the lake. In many places, they constitute a kind of ecotone zone to the organic soils located at the lowest elevations, slightly above the current water table of Jeziorak. In drawing the boundary between semihydrogenic soils and higher-located well-drained soils, the terrain model proved to be very useful. Isohypsies located at heights of 100–103 m a.s.l. were used here. Differences in these heights result from local differentiation determined by topography. The foot of long and steep slopes may be more strongly supplied with intra-surface groundwater, which slightly raises the upper altitude limit of the occurrence of semihydrogenic soils.

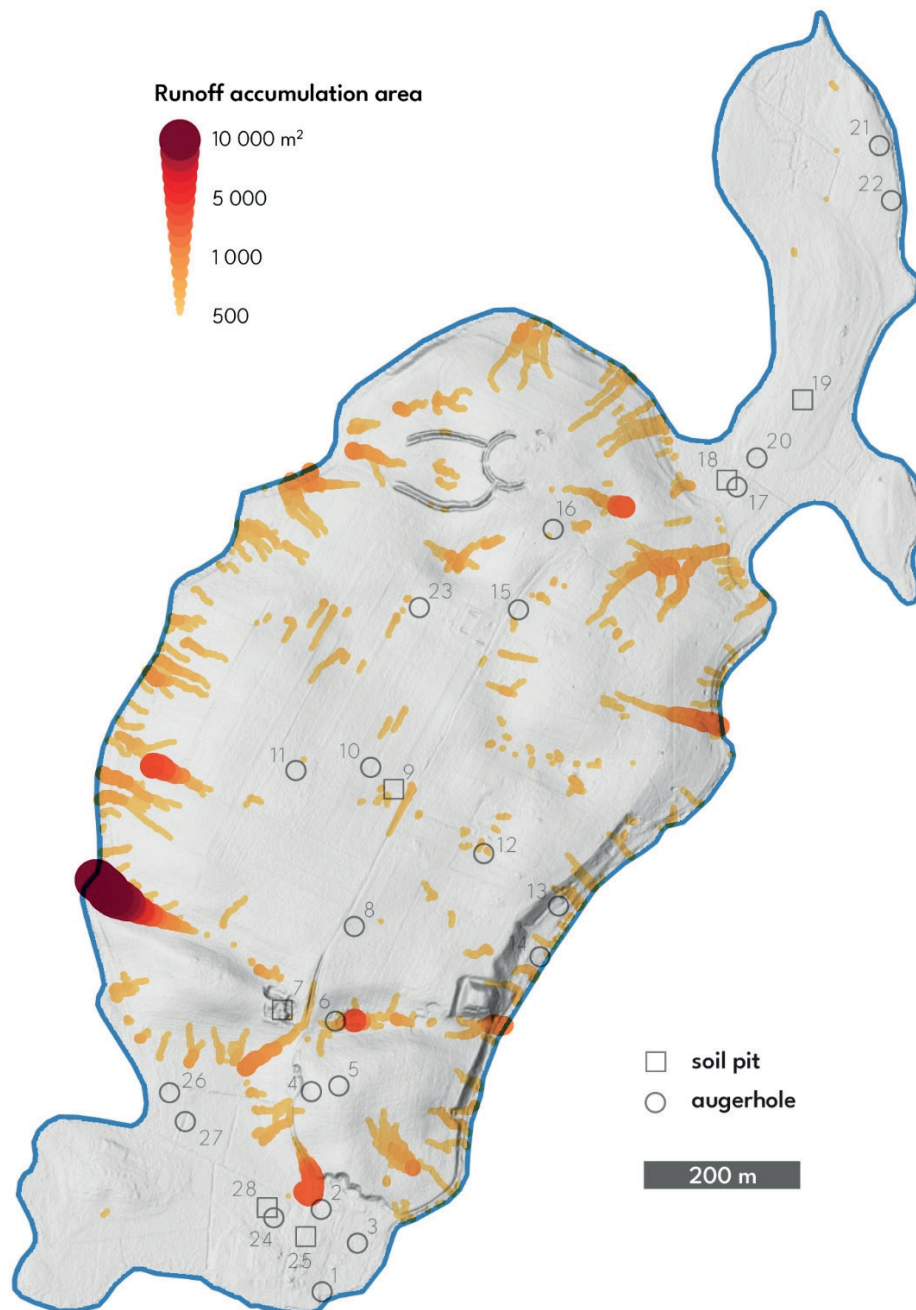


Fig. 6. Map of the potential runoff on Wielka Żuława

The digital terrain model was also successfully used to determine the boundary between organic (peat and murshic soils – PSC 2019; or Histosols according to WRB) and mineral semihydrogenic soils. Fieldworks confirmed that, regardless of the part of the island, this boundary runs at an altitude of ~100 m a.s.l. All profiles of organic soils examined in the field showed clear signs of degradation, visible in the form of mursh, i.e. black organic matter with

a granular structure (Okruszko 1976, 1993; Roguski 1980; Piaścik and Gotkiewicz 1995). The thickness of this mursh ranged from several centimetres to more than one metre. During the analysis of the DTM based on LiDAR data (i.e., “after removing” the data on vegetation cover), it was noticed that heavily degraded soils (with muck of over 30 cm thick) occur in the northernmost and southern parts of island (areas with visible drainage channels) (Fig. 7).



Fig. 7. Application of the relief model in determining the presence of mucky soils based on visible networks of drainage ditches: visualisation using DEM and Sky View Factor analysis, based on GUGIK data

These channels were poorly visible at the stage of fieldworks and are currently not clearly visible on the orthophotomap, mainly due to the dense alder forests growing on organic soils. LiDAR data revealed the impact of humans on drainage and degradation of organic soils, which made it possible to separate murshic from peat soils on the elaborated map of soil cover.

The last issue, in which both aerial photos and DTM were used, was determining the range of technogenic soils – those related to the occurrence of both earthen structures and infrastructure created

by man. The result of such activity is technogenic soils (urbisols, ekranosols, turbisols, aggerosols) whose largest ranges of occurrence were confirmed in the eastern and southern parts of the island, where holiday resorts were located in the past. LiDAR data allowed even for the precise determination of the extent of a “stronghold” created for the filming of the movie *The Nest* in the 1970s (Fig. 8).

5. Conclusions

The conducted research allows for the formulation of the following conclusions:

- The island of Wielka Żuława is dominated by clay-illuvial and rusty soils (Luvisols and Brunic Arenosols – WRB) developed from kame deposits. Separating these soils on the map is not possible due to the varied and dynamically changing thickness of the sandy cover and the depth of loam (and the top of the Bt horizon). This interchangeability is not reflected in any available cartographic materials;
- In the northern and southern parts of the island there are large areas of organic pedons – peat and murshic soils (Histosols or Murshic Histosols – WRB);
- The relief model elaborated on the basis of LiDAR data shows networks of drainage ditches and turned out to be very useful in determining the extent of murshic soils (Murshic Histosols – WRB 2022) resulting from anthropogenic drainage and degradation of peat soils;
- The relief model made it possible to quite precisely determine the boundary between organic soils and mineral soils with poor natural drainage: black earths (Endogleyic Phaeozems or Mollic Gleysols in WRB); it runs at an altitude of 100 m a.s.l.;
- Some difficulties were encountered in determining the transition from the above-mentioned soils with natural poor drainage (black earths) to well-drained pedons (clay-illuvial and rusty soils). Depending on the topography of the land, it is located at an altitude of 100.5 to 102 m a.s.l.;
- The landform model combined with an archival orthophotomosaic (showing the historical



Fig. 8. Remains of the "stronghold" from the film The Nest

extent of arable land) was used to determine places of possible occurrence of colluvial soils;

- The archival orthophotomosaic together with a relief model allowed for the selection of places where technogenic soils (WRB – Technosols) occur (i.e., turbisols, aggerosols, urbisols, ekranosols).

The next stage of the work should be the evaluation of the obtained results, especially in the context of erosional transformations of the soil cover and the range of other forms of impact of human activity.

Acknowledgment

The analyses were performed in The Laboratory for Environmental Analysis (LEA), Faculty of Earth Sciences and Spatial Management of Nicolaus Copernicus University in Toruń.

Disclosure statement

No potential conflict of interest was reported by the authors.

Author contributions

Study design: MŚ, MM; data collection: MŚ, MM, JD, PR, MS; statistical analysis: MŚ, MM; result interpretation: MŚ, MM, JD, PR, MS; manuscript preparation: MŚ, PR, JD; literature review: MŚ, PR.

References

- AKAMIGBO FOR, IGWE CA and ORANEKWULU SC, 1994, Soil variability in map units delineated by aerial photo-interpretation: a case study in Anambra State, Nigeria. *Soil Use and Management* 10: 6–8. DOI: <https://doi.org/10.1111/j.1475-2743.1994.tb00449.x>.
- BAURLEY NR, TOMSETT C and HART JK, 2022, Assessing UAV-based laser scanning for monitoring glacial processes and interactions at high spatial and temporal resolutions. *Frontiers in Remote Sensing*, 3: 1027065.
- BIAŁOUSZ S, 1978, Zastosowanie fotointerpretacji do wykonywania map stosunków wodnych gleb. *PTG, Prace Komisji Naukowych* 35: 1–143.
- BIAŁOUSZ S, MIROSZ K and SIMLA M, 1978, Wpływ wilgotności gleby na zróżnicowanie tonu zdjęcia lotniczego. *Fotointerpretacja w geografii* 12: 111–116.
- BURINGH P, 1970, *Introduction to the study of soils in tropical and subtropical regions*. PUDOC, Wageningen.
- DE FEUDIS M, FALSONE G, GHERARDI M, SPERANZA M, VIANELLO G and ANTISARI LV,

- 2021, GIS-based soil maps as tools to evaluate land capability and suitability in a coastal reclaimed area (Ravenna, northern Italy). *International Soil and Water Conservation Research* 9(2): 167–179.
- DOMLIJA P, GAZIBARA SB, ARBANAS Ž and ARBANAS SM, 2019, Identification and Mapping of Soil Erosion Processes Using the Visual Interpretation of LiDAR Imagery. *ISPRS International Journal of Geo-Information* 8(10): 438. DOI: <https://doi.org/10.3390/ijgi8100438>.
- GUNAY CJC, MAGCALE-MACANDOG DB and BRAGAIS MA, 2019, Assessing soil erosion and flood risk areas in Santa Rosa-Silang Watershed using LiDAR data and SWAT modeling. *Sylvatrop, The Technical Journal of Philippine Ecosystems and Natural Resources* 29, (2): 23–38.
- GEVAERT CM, SUOMALAINEN J, TANG J and KOOISTRA L, 2015, Generation of Spectral-Temporal Response Surfaces by Combining Multispectral Satellite and Hyperspectral UAV Imagery for Precision Agriculture Applications. *IEEE Journal of Selected Topics in Applied Earth Observations* 8: 3140–3146.
- INTERGOVERNMENTAL PANEL ON CLIMATE CHANGE (IPCC), 2006, IPCC Guidelines for National Greenhouse Gas Inventories. Volume 4. Egglestone HS, Buendia L, Miwa K, Ngara T and Tanabe K (eds), *Intergovernmental Panel on Climate Change (IPCC), IPCC/IGES*. Hayama, Japan.
- IUSS WORKING GROUP WRB, 2022, World Reference Base for Soil Resources. International soil classification system for naming soils and creating legends for soil maps. 4th edition. *International Union of Soil Sciences (IUSS)*. Vienna, Austria.
- JONG-TAE K, JUNG-HYUN K, CHANG-HUN L, SEONG-CHEOL P, CHANG-JU L and GYO-CHEOL J, 2023, Monitoring Landcreep Using Terrestrial LiDAR and UAVs. *The Journal of Engineering Geology* 33(1): 27–37.
- KABAŁA C, CHARZYŃSKI P, CHODOROWSKI J, DREWNIK M, GLINA B, GREINERT A, HULISZ P, JANKOWSKI M, JONCZAK J, ŁABAZ B, ŁACHACZ A, MARZEC M, MENDYK Ł, MUSIAŁ P, MUSIEŁOK Ł, SMRECZAK B, SOWIŃSKI P, ŚWITONIAK M, UZAROWICZ Ł and WAROSZEWSKI J, 2019, Polish Soil Classification, 6th edition – principles, classification scheme and correlations. *Soil Science Annual* 70(2): 71–97. DOI: <https://doi.org/10.2478/ssa-2019-0009>.
- KOBIERSKI M, 2013, *Morphology, properties and mineralogical composition of eroded Luvisols in selected morainic areas of the Kujavian and Pomeranian Province*. University of Technology and Life Sciences, Bydgoszcz.
- KOTTEK M, GRIESER J, BECK C, RUDOLF B and RUBEL F, 2006, World Map of Köppen-Geiger Climate Classification updated. *Meteorologische Zeitschrift* 15(3): 259–263.
- MALIK RP, SHANWAL AV and IYER HS, 1984, Identification and delineation of saline soils using aerial photographs in Yamuna Alluvial plain, Haryana. *Journal of the Indian Society of Photo-Interpretation and Remote Sensing* 12: 59–64. DOI: <https://doi.org/10.1007/BF02991438>.
- MARKS L, 2012, Timing of the Late Vistulian (Weichselian) glacial phases in Poland. *Quaternary Science Reviews* 44: 81–88.
- MATECKA P and ŚWITONIAK M, 2020, Delineation, characteristic and classification of soils containing carbonates in plow horizons within young moraine areas. *Soil Science Annual* 71(1): 23–36. DOI: <https://doi.org/10.37501/soilsa/121489>.
- OKRUSZKO H, 1976, Effect of land reclamation on organic soils in Poland's conditions. *Zeszyty Problemowe Postępów Nauk Rolniczych* 177: 159–204.
- OKRUSZKO H, 1993, Transformation of fen-peat soils under the impact of draining. *Zeszyty problemowe postępów nauk rolniczych* 406: 3–73.
- PHILLIPS JD, SLATTERY MC and GARES P A, 1999, Truncation and accretion of soil profiles on coastal plain croplands: implications for sediment redistribution. *Geomorphology* 28(1): 119–140. DOI: [https://doi.org/10.1016/S0169-555X\(98\)00105-6](https://doi.org/10.1016/S0169-555X(98)00105-6).
- PIAŚCIK H and GOTKIEWICZ J, 1995, Degradation processes on the drained peatlands of the post-glacial areas. *Zeszyty problemowe postępów nauk rolniczych* 418: 185–190.
- PODLASIŃSKI M, 2013, *Denudation of anthropogenic impact on the diversity of soil cover and its spatial structure in the agricultural landscape of moraine*. Szczecin.
- POLSKIE STOWARZYSZENIE KLASYFIKATORÓW GRUNTÓW, 2020, *Szczegółowe zasady przeprowadzania gleboznawczej klasyfikacji gruntów*. Puławy – Warszawa.
- POLISH SOIL CLASSIFICATION, 2019. *Soil Science Society of Poland, Commission on Soil Genesis, Classification and Cartography*. Wydawnictwo Uniwersytetu Przyrodniczego we Wrocławiu, Polskie Towarzystwo Gleboznawcze, Wrocław – Warszawa.

- RADZIUK H and ŚWITONIAK M, 2022, The Effect of Erosional Transformation of Soil Cover on the Stability of Soil Aggregates within Young Hummocky Moraine Landscapes in Northern Poland. *Agronomy* 12(11): 2595. DOI: <https://doi.org/10.3390/agronomy12112595>.
- REDDY AD, HAWBAKER TJ, WURSTER F, ZHU Z, WARD S, NEWCOMB D and MURRAY R, 2015, Quantifying soil carbon loss and uncertainty from a peatland wildfire using multi-temporal LiDAR. *Remote Sensing of Environment* 170: 306–316.
- ROGUSKI W, 1980, Przemiany gleb organicznych w Dolinie Noteci w wyniku wieloletniego użytkowania rolniczego i ich właściwości fizyczno-wodne. *Roczniki gleboznawcze* 31(3/4): 109–115.
- SABOL J, PATOČKA Z and MIKITA T, 2014, Usage of LiDAR data for leaf area index estimation. *GeoScience Engineering* 60(3): 10–18.
- SINGH D, HERLIN I, BERROIR JP, SILVA EF and SIMOES MEIRELLES M, 2004, An approach to correlate NDVI with soil colour for erosion process using NOAA/AVHRR data. *Advances in Space Research* 33(3): 328–332.
- SINKIEWICZ M, 1998, *The development of anthropogenic denudation in central part of northern Poland*. Nicolaus Copernicus University, Toruń.
- SOLAZZO D, SANKEY JB, SANKEY TT and MUNSON SM, 2018, Mapping and measuring aeolian sand dunes with photogrammetry and LiDAR from unmanned aerial vehicles (UAV) and multispectral satellite imagery on the Paria Plateau, AZ, USA. *Geomorphology* 319: 174–185.
- ŚWITONIAK M, 2006, Different pedogenesis conditioned by lithology of texture-contrast soils in Brodnica Lake District. In: Gierszewski P, Karasiewicz M (eds), *Ideas and practical universalism of geography. Geographical documentation* 32: 278–285.
- ŚWITONIAK M, 2007, Ocena wartości ekologicznej gleb o dwudzielnym uziarnieniu w aspekcie zrównoważonego gospodarowania obszarami leśnymi Brodnickiego Parku Krajobrazowego. In: Marszelewski W, Kozłowski L (eds), *Ochrona i zagospodarowanie Drwęcy. Vol. 1*. Toruń, 335–344.
- ŚWITONIAK M, 2014, Use of soil profile truncation to estimate influence of accelerated erosion on soil cover transformation in young morainic landscapes, North-Eastern Poland. *Catena* 116: 173–184.
- ŚWITONIAK M, 2015, Issues relating to classification of colluvial soils in young morainic areas (Chełmno and Brodnica Lake District, northern Poland). *Soil Science Annual* 66(2): 57–66.
- ŚWITONIAK M, MARKIEWICZ M, BEDNAREK R and PALUSZEWSKI B, 2013, Application of aerial photographs for the assessment of anthropogenic denudation impact on soil cover of the Brodnica Landscape Park plateau areas. *Ecological Questions* 17: 101–111.
- ŚWITONIAK M, MROCZEK P and BEDNAREK R, 2016, Luvisols or Cambisols? Micromorphological study of soil truncation in young morainic landscapes — Case study: Brodnica and Chełmno Lake Districts (North Poland). *Catena* 137: 583–595.
- TOMCZYK A and BEDNORZ E, 2022. *Atlas klimatu Polski (1991–2020)*. Bogucki Wydawnictwo Naukowe.
- ZÁDOROVÁ T, PENÍŽEK V, KOUBOVÁ M, LISÁ L, PAVLŮ L, TEJNECKÝ V, ŽIŽALA D, DRÁBEK O, NĚMEČEK K, VANĚK A and KODEŠOVÁ R, 2023, Formation of Colluvisols in different soil regions and slope positions (Czechia): Post-sedimentary pedogenesis in colluvial material. *Catena* 229: 107233. DOI: <https://doi.org/10.1016/j.catena.2023.107233>.
- ŽIŽALA D, JUŘICOVÁ A, ZÁDOROVÁ T, ZELENKOVÁ K and MINAŘÍK R, 2019, Mapping soil degradation using remote sensing data and ancillary data: South-East Moravia, Czech Republic. *European Journal of Remote Sensing* 52(1): 108–122. DOI: <https://doi.org/10.1080/22797254.2018.1482524>.
- ZHOU J, XU Y, GU X, CHEN T, SUN Q ZHANG S and PAN Y, 2023, High-Precision Mapping of Soil Organic Matter Based on UAV Imagery Using Machine Learning Algorithms. *Drones* 7: 290. DOI: <https://doi.org/10.3390/drones7050290>.

Received 25 October 2024
Accepted 9 December 2024